JOURNAL OF AGRICULTURAL AND FOOD CHEMISTRY
ARTICLE

J. Agric. Food Chem. 2009, 57, 11383–11390 11383
DOI:10.1021/jf902638e

Novel Anticancer Activity of the Autocleaved Ovotransferrin against Human Colon and Breast Cancer Cells

HISHAM R. IBRAHIM*,† AND TOHRU KIYONO§

†Department of Biochemistry and Biotechnology, Faculty of Agriculture, Kagoshima University, Kagoshima 890-0065, Japan, and §Virology Division, National Cancer Center Research Institute, Chuo-ku, Tokyo, 104-0045, Japan

Proteins of avian egg albumin have been suggested to play various biological roles during the development of chick embryo to confer protection. Recently, we have shown that ovotransferrin (OTf), the second major protein in egg albumin, undergoes thiol-linked autocleavage at distinct sites upon reduction. This study explores the physiological significance of OTf autocleavage by examining the effect of the reduced autocleaved OTf (termed rac-OTf) on modulation of cell proliferation, lethality, and apoptosis in two human cancer cell lines, colon cancer (HCT-116) and breast cancer (MCF-7). The rac-OTf was prepared by reduction of OTf with a non-thiol reductant (TCEP), to avoid reductive alkylation and produce highly soluble fragments. Unlike OTf, rac-OTf remarkably inhibited the proliferation of cancerous MCF-7 and HCT-116 cells in a dose-dependent manner, with the greatest effect on HCT-116, but had no effect on normal human mammary epithelial cells (HMEC). Cytofluorometric and trypan blue exclusion analyses indicated that rac-OTf exhibits cytotoxicity to HCT-116 in a dose-dependent fashion. The cytotoxic mechanism of rac-OTf against cancer cells was found to be induction of apoptosis as judged by changes in cell morphology, annexin-V binding, collapse of mitochondrial membrane potential, and caspase-9 and -6 activation, indicating the involvement of the mitochondrial pathway. This finding is the first to describe the reduction-dependent autocleaved OTf as an anticancer molecule, providing insights into a novel physiological function of OTf, suggesting its therapeutic potential in the treatment of human cancers and health benefit in nutraceuticals.

KEYWORDS: Ovotransferrin; hen egg albumin; autocleavage; kringle domain; tumoricidal activity; colon cancer; breast cancer; apoptosis; anticancer peptide therapy; bio-active peptides

INTRODUCTION

Eggs are biological reactors that contain all necessary molecules to produce chick life and thus represent an excellent example of nature's original functional food. Particularly, egg albumen is loaded with many bioactive proteins, which intriguingly interact to protect the chick embryo, that are known to promote optimal health and have long been thought to play important roles in disease prevention and health promotion. However, the biological functions of key proteins of egg albumen are still poorly understood. Hence, we are facing a big challenge to uncover the biological activities of key proteins of egg albumen as well as the basis of their molecular activation and to formulate novel candidates for health foods and therapy.

Recent studies identified several proteins involved in complex biological processes that have more than one function in an organism (*1*, *2*). This was partially attributed to the apparent ability of several proteins to self-proteolyze as a way to activate themselves and thus have multiple functions within one polypeptide chain. This posttranslational modification, that is, autocleavage, includes proteins with different types of functions within different organisms from microorganisms to man (*3*−*5*). Autocleavage of proteins was found to be necessary for diverse biological processes such as regulation of blood pressure, cell cycle, development, apoptosis, and cytoprotection (*3*, *4*). Most of these autocleavage processes are redox-regulated, particularly under reducing conditions (*6*−*8*). These include disulfide reduction-induced autocleavage of hedgehog proteins (*4*) and milk plasminogen (*6*) that are known to play pivotal roles in the development of embryos and conversion to antitumor molecule, respectively.

The profound clue that protein disulfide manipulation plays a role in tumor pathology came from studies that identified antitumor disulfide kringle domains (angiostatins) of plasminogen found in milk and other secretions (*9*, *10*). Angiostatin consists of kringles 1−4 (K1−4) plus 85% of kringle 5 (K5) of plasminogen. The antitumor activation occurs through the reduction of one or more disulfide bonds within plasmin(ogen) by a reductase secreted by cancer cells PC-3, HT1080, HCT 116, and MDA-MB231 (*10*, *11*) or by a free sulfhydryl donor such as dithiothreitol (DTT) (*6*). In addition to the K1−4 species (generated by plasmin autoproteolysis under reducing condition), disulfide kringles K1−5 and angiostatin K1−3 have also been identified. All of these angiostatin-related kringle domains exert similar

*Author to whom correspondence should be addressed [telephone +81 (99) 285-8656; fax +81 (99) 285-8525; e-mail hishamri@chem.agri.kagoshima-u.ac.jp].

Published on Web 11/03/2009

antitumor activities including apoptosis induction with various degrees of effectiveness (*12*).

Among the disulfide kringle-containing proteins, ovotransferrin (OTf) is a major protein in hen egg albumin with a molecular mass of 78 kDa (686 residue), containing 15 disulfide cross-links (*13*). OTf belonging to the transferrin (Tf) family include serum transferrin (Tf), milk lactoferrin (Lf), and avian OTf. The global structures of OTf and Tfs are identical, differing only in the nature of their attached glycan chain and their p*I* values (*13*). Besides the implication in the transport of iron to the target cells, Tfs are proposed to be involved in a large number of cellular events in which they act as event triggers or receptor activators. These physiological processes include the stimulation of cell proliferation (*14*), tumoral processes (*15*, *16*), and promotion of endothelial cell invasion (*17*). OTf expression level in chicken serum also increases in inflammation and infection (*18*).

As far as "anti-tumor disulfide kringle modules" are concerned, we have recently shown that reduction with thioredoxin or DTT triggered autocleavage of OTf, thus releasing its two kringle modules (*19*). The reduction-dependent autocleavage of OTf occurred primarily at four distinct sites flanking the two disulfide kringles, leading to the liberation of the two kringle domains and fragments containing different NH_2 and COOH termini (*19*).

The accumulating evidence indicates that OTf seems always to be associated with processes involving redox-related signals. Particularly, it is known that redox imbalance as a result of dependence on "aerobic glycolysis" rather than "respiration" is a universal property of malignant cells, and it has been suggested that cancer is caused by impaired mitochondrial metabolism (*20*). Alterations in the respiratory function have been associated with an increase in the mitochondrial energy metabolism or reactive oxygen species (ROS) production (*21*). A selectively cleaved form of OTf was found to be induced by oxidative inflammation in macrophage of goldfish (*22*) and chicken (*18*). Human and bovine lactoferrins were shown to inhibit tumor-induced angiogenesis (*23*) and to suppress tumor growth and metastasis (*16*, *24*−*26*). Furthermore, tumor cells generally have higher levels of transferrin receptor-1 (TfR1) than their normal counterparts (*27*). Lactoferrin was also found to be associated with neurodegenerative disorder (*28*). The individual kringle (K1−4 and K5) domains released from human plasmin(ogen) upon reduction, which exhibit antiproliferative activity (*29*), have been shown to share structural similarity with the kringle pockets of OTf (*13*). In our recent studies we observed that OTf exposed to reducing condition undergoes conformational changes in the vicinity of its two kringle regions and is subsequently autocleaved (*19*), whereas the autocleaved OTf was found to possess superoxide dismutase (SOD)-like activity (*30*). SOD is an important antioxidant enzyme that has recently been found to inhibit cancer cells (*31*). Protein antioxidant-defense activation processes are often triggered by redox modification of a cysteine side chain, which is known to play a major role in redox sensing and the antioxidant response of SOD (*32*). Therefore, thiol-specific modification at key cysteine residues may be the molecular switch in generating various kringle forms of OTf with particular effect on cellular functions. Specifically, we anticipate that the reduced autocleaved form of OTf may confer antiproliferative activity toward cancer cells in a fashion similar to the multifunctional plasminogen.

It is the purpose of this study to examine the effect of reduction-induced autocleavage of OTf on the viability of cancer cells. For this, a non-thiol reducing agent, TCEP, was employed to reduce OTf under acidic condition to avoid DTT reduction-induced aggregation. In this study, we present the first demonstration that the reduced auto-cleaved OTf (termed rac-OTf) selectively inhibits proliferation and induces apoptosis of human colon (HCT-116) and breast (MCF-7) cancer cells.

MATERIALS AND METHODS

Materials. Ovotransferrin, purchased from Inovatech BioProducts Inc. (Abbotsford, Canada), was recrystallized and chromatographically (Sephadex G-50) purified to >98% as judged by its extinction coefficient at 280 nm and Western blotting using polyclonal antibody. Sephadex G-25 was a product of Amersham-Pharmacia Biotech (Tokyo, Japan). Fetal bovine serum (FBS), phosphate-buffered saline (PBS), dimethyl sulfoxide (DMSO), trypan blue (TB), propidium iodide (PI), protease inhibitors cocktail, and tris(2-carboxyethyl)phosphine (TCEP) were from Sigma (St. Louis, MO). Camptothecin was from Funakoshi (Tokyo, Japan). E-MEM medium, McCoy 5a medium, nonessential amino acids, and sodium pyruvate were from ICN (Costa Mesa, CA). The CyQuant cell proliferation assay kit (C-7026) and the Live/Dead viability/cytotoxicity kit (L-3224) for animal cells were from Molecular Probes (Invitrogen Japan, Tokyo). The ApoAlert annexin V-EGFP apoptosis kit (K-2019) and ApoAlert caspase-9/6 fluorescent assay kit (K-2015) were from BD Pharmingen (San Diego, CA). The mitochondria permeability detection kit (AK-116) was from BioMol (Allemagne, Germany). Unless otherwise stated, all other chemicals were of analytical grade.

Cell Lines and Cultures. Human breast cancer MCF-7 (ATCC HTB-22) and human colon cancer HCT-116 (ATCC CCL-247) cell lines were obtained from American Type Culture Collection (Rockville, MD). Normal primary human mammary epithelial cells HMEC (immortalized with ectopic expression of human telomerase reverse transcriptase, hTERT) were a kind gift from the National Cancer Center Research Institute (Tokyo, Japan). MCF-7 and HCT-116 cells were maintained in E-MEM media (with nonessential amino acids and sodium pyruvate) and McCoy's 5a media, respectively, both supplemented with 10% fetal bovine serum (FBS) and antibiotics (penicillin and streptomycin). HMEC cells were maintained in MEGM Bullet kit (Takara, Tokyo, Japan) containing the following: epithelial cells basal medium (MEBM), bovine pituitary extract, hydrocortisone, human epidermal growth factor, insulin, and antibiotics with 1% FBS. Working cultures were maintained at 37 °C in a humidified incubator with 5% CO_2, and the medium was changed every other day.

Preparation of the Reduced Autocleaved OTf (rac-OTf). The reduced autocleaved form of OTf was prepared by reduction with 0.2 mM TCEP in 20 mM citrate−phosphate, pH 4.0, for 6 h at 37 °C. The reaction was followed by Sephadex G-25 gel filtration chromatography (NAP-5, Pharmacia Biotech Inc.) to remove TCEP. Protein peak was dialyzed (3 kDa cutoff) against distilled water and centrifuged (5000*g* for 10 min), and the resulting supernatant was freeze-dried. The pH profile of reduction-induced autocleavage of OTf was assessed in 20 mM McIlvaine buffer, pH 3.0−8.0, containing 0.2 mM TCEP or DTT and 10 μM OTf for 6 h at 37 °C. The TCEP- and DTT-induced autocleavage of OTf was analyzed on nonreducing and reducing SDS-PAGE.

Cell Proliferation Assay. Proliferation of HMEC, MCF-7, and HCT-116 cells was determined with the CyQuant Cell Proliferation Assay kit. Cells were seeded at 2500 cells/cm^2 in the appropriate medium and incubated at 37 °C for 24 h without treatment. Cells were treated by changing the culture medium with a medium containing different concentrations of OTf or rac-OTf (0−1000 μg/mL) and incubated at 37 °C for 48 h. The CyQuant assay was performed according to the manufacturer's instructions. After addition of the CyQuant Dye solution to the freeze−thawed cell pellets, fluorescence was measured from four parallel wells per sample at excitation and emission of 485 and 538 nm, respectively, in an automated microplate fluorometer, Fluoroskan Ascent FL (Labsystems, Helsinki, Finland) with on-board software. After subtraction of controls and blank values from each sample, relative fluorescence units (RFU) read-outs, of two independent experiments, were used to calculate the proliferation index according to the following formula:

$$\text{proliferation index} = \text{RFU treated cells} \times (1/\text{RFU mock cells})$$

Cytotoxicity Assay. The viability of HCT-116 cells (2.0×10^6 cells/mL) treated for 4 h with OTf or rac-OTf was determined using the trypan blue (0.2% TB solution) exclusion test. The percentage of dead cells is calculated as (number of stained cells/number of total cells) × 100.

The viability of HCT-116 cells treated with rac-OTf was also determined using a highly sensitive assay, the Live/Dead viability/cytotoxicity kit (Molecular Probes). The kit contains two components, calcein-AM (cal-AM) and ethidium homodimer (EthD-1). Calcein-AM penetrates the membrane of live (vital) cells, whereas esterases in the cytoplasm render it fluorescent (green). Ethidium homodimer is not able to penetrate intact cell membranes but adheres to nucleic acids of damaged (dead) cells (red fluorescent cells). The cells (8.0×10^6 cells/mL) were treated for 4 h with different concentrations of rac-OTf. Dead cells subjected to 75% ethanol killing for 1 h were used as a positive control. The cells were stained with the dye solution in a 96-well black fluoroplates, and the fluorescence intensity was measured by excitation at 485 nm and detection at 642 nm (red) and 538 nm (green). Live and dead cells were presented as differential staining of the green RFU (stains all cells, live or dead) and the red RFU (stains only dead cells). Intensities were calculated from four parallel wells per sample after subtraction of controls and blank values from each sample. The treated cells were also photodocumented, before and after detachment, by phase contrast microscopy.

Annexin-V and PI Apoptosis Assay. Apoptosis was analyzed by double-fluorescence staining methods of cells with annexin V−EGFP and PI, using a microplate fluorometer and an inverted fluorescent microscope. Labeled annexin-V enables visualization of cells in the early- to mid-apoptotic state. The HCT-116 cells were treated for 3.5 h with rac-OTf (250 μg/mL) or camptothecin (4 μg/mL), as a positive apoptosis control, washed in PBS, and stained with EGFP conjugated annexin-V or PI. The cells were washed twice with binding buffer and then analyzed by the Fluoroskan Ascent FL fluorescence microplate reader by excitation at 485 nm and detection at 590 nm (PI, red RFU) and 538 nm (annexin V, green RFU). Fluorescent intensities were calculated from four parallel wells per sample after subtraction of controls and blank values from each sample. Cells were also examined with an inverted fluorescent microscope (Olympus CKX41, Olympus Optical Inc., Tokyo, Japan). Images of various fields in each well were captured at 10× magnification.

Measurement of Mitochondrial Membrane Potential ($\Delta\Psi_m$). The $\Delta\Psi_m$ was measured with the mitochondria permeability detection kit, by using the cationic fluorescent dye, JC-1 (BioMol, Allemagne, Germany). The HCT-116 cells were treated with rac-OTf (250 μg/mL) or camptothecin (4 μg/mL) in McCoy 5a medium for 3.5 h. At the end of treatments, the culture medium was removed and the cells were loaded with 1× dye in assay buffer for 15 min at 37 °C in a 5% CO_2 incubator in 24-well plates. Cells were rinsed twice with assay buffer, and fluorescent intensities were measured from four parallel wells per sample by a Fluoroskan Ascent FL fluorescence microreader by excitation at 485 nm and emission at 590 nm (red) and 538 nm (green). After subtraction of controls and blank values from each sample, relative fluorescence units (RFU) read-outs were used to calculate the dissipation of mitochondria potential expressed as green/red RFU ratios. Cells were also examined with an Olympus inverted fluorescent microscope (Olympus CKX41), excited at 485, Em = 525 (for JC-1 green) and Em = 590 (for JC-1 red). Images of various fields in each well were captured with the digital camera at 10× magnification.

Assessment of Caspase-9/-6 Activities. Intracellular activity of caspase-9 and -6 was measured using a fluorometric assay kit (BD Biosciences) according to the manufacturer's instructions. In brief, the HCT-116 and MCF-7 cells treated with OTf, rac-OTf (250 μg/mL), or camptothecin (4 μg/mL) in culture medium for 24 h were lysed to collect their intracellular contents. A 50 μL portion of the cell extracts was added to 57 μL of reaction mixture consisting of 2× assay buffer and substrate (LEHD-AMC) with and without caspase inhibitor, incubated at 37 °C for 1 h in a 96-well black fluoroplate. The release of aminomethylcoumarin was measured, from three parallel wells per sample, using a Fluoroskan Ascent FL fluorescence microreader (excitation at 380 nm and emission at 460 nm). A portion of the cells was loaded into a hemocytometer and counted under a microscope for estimation of total cell count per treatment. The catalytic activities are expressed as relative fluorogenic units (RFU) per 10^6 cells and as fluorescence change over control.

RESULTS

TCEP Generates Highly Resolved OTf Autocleavage Fragments. Recently, we have shown that thioredoxin is a natural reductant for OTf self-catalyzed cleavage, whereas DTT can be used as the in vitro reductant. However, the autoproteolytic fragments produced by the dithiol DTT lacked resolved Cys residues, and insoluble OTf aggregate was predominant (*19*). In addition, DTT is known to be inactive as a reducing agent at acidic pH. To explore the biological role of the OTf autoprocessing, autocleavage was induced by a non-thiol reductant (TCEP) to avoid reductive alkylation and produce soluble fragments. As shown in Figure **1**, compared to the low-resolution bands produced by DTT (**Figure 1B**), TCEP induced autocleavage of OTf into many fragments at neutral and alkaline pH values and specifically at pH 4.0 produced a slightly lesser number of bands but with higher intensities and good resolution (**Figure 1Aa**,**b**). In addition, TCEP-induced autocleavage OTf was completely soluble at any pH condition, whereas TCEP-induced autocleavage did not cause changes in the absorbance (at 500 nm) of the OTf solution. Interestingly, TCEP-induced autocleavage OTf at pH 4.0, but not DTT reduction, showed clear bands with similar autoproteolytic patterns when resolved on either reducing or nonreducing SDS-PAGE (**Figure 1Ba**,**b**), indicating the lack of scrambled intermolecular disulfides.

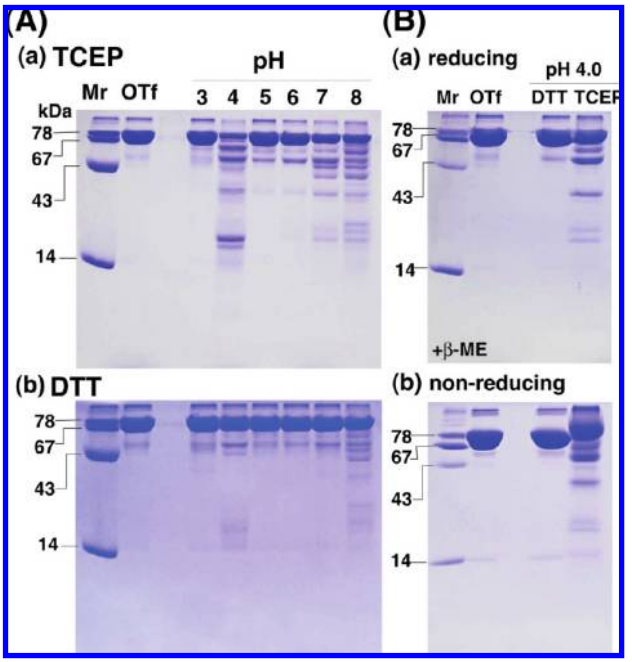

Figure 1. Electophoretic patterns of reduction-induced autocleavage of OTf: (**A**) pH profile of the autocleavage of OTf incubated with 200 μM TCEP (**a**) or DTT (**b**) at 37 °C for 6 h at different pH values (pH 3.0−8.0); portions were then applied to SDS-PAGE; (**B**) portion of OTf reduced at pH 4.0 by either TCEP (rac-OTf) or DTT applied to a reducing (**a**) or nonreducing (**b**) SDS-PAGE.

It is well-known that the extracellular pH of tumors is acidic and that the proton pump (H^+-ATPase) at the plasma membrane contributes to the maintenance of such acidic pH (*33*, *34*). In parallel, cancer cells are known for their high secretion of disulfide-reducing agents and enzymes (*35*, *36*). Hence, we anticipate that the reduced autocleaved form of OTf may confer antiproliferative activity toward cancer cells in a fashion similar to the multifunctional plasmin (*9*, *10*). Therefore, the autocleaved OTf prepared under acidic condition (termed rac-OTf) was used in the following cell-based antitumor bioassays against two different cancer cells, HCT-116 and MCF-7, known for their overexpression of a thioredoxin−thioredoxin reductase system and extracellular acidic pH (*33*, *37*, *38*).

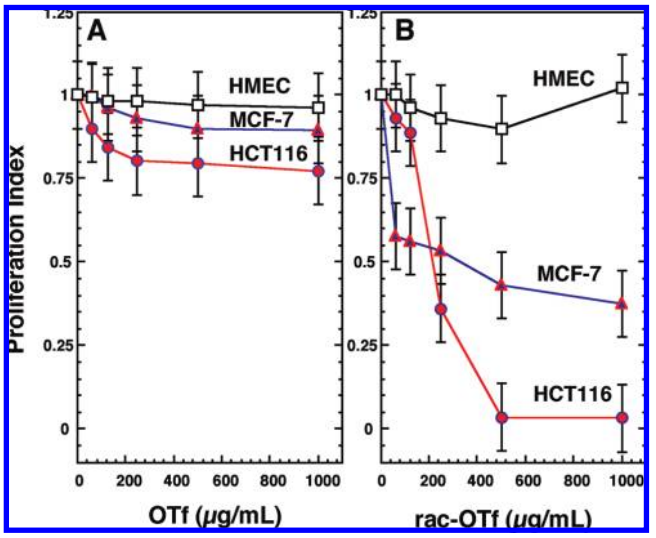

Figure 2. Antiproliferative activity of OTf (**A**) and rac-OTf (**B**) against human colon (HCT-116) and human breast (MCF-7) carcinoma cells in comparison with its effect on normal human mammary epithelial cells (HMEC). Cells cultured for 24 h were treated by different concentrations of protein (0−1000 μg/mL) and incubated at 37 °C for 48 h. The CyQuant proliferation assay was performed in a fluoromicroplate by measuring fluorescence at excitation and emission of 485 and 538 nm, respectively. Proliferation index was calculated as described under Materials and Methods. Values shown represent the mean of two experiments from four parallel wells per sample in each experiment.

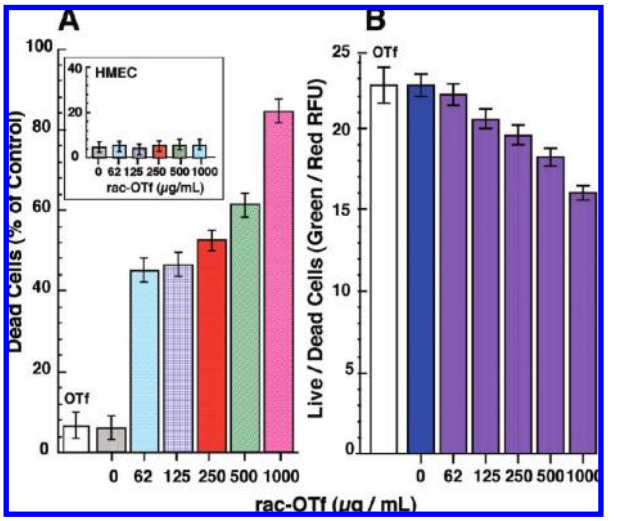

Figure 3. Viability of human colon cancer HCT-116 cells treated with rac-OTf assessed by trypan blue exclusion (**A**) and live/dead fluoroassay (**B**). Cells were pretreated for 4 h with intact OTf or different concentrations of rac-OTf. Total cell count was obtained by hemocytometer count under a microscope. In (**A**) the dead cells were estimated as [number of TB positive cells/number of total cells] × 100. The inset shows the viability of normal human HMEC cells treated with rac-OTf. In (**B**) the cytotoxicity is represented as a ratio of green (live)/red (dead) fluorescence. In both assays, treatment with rac-OTf resulted in a statistically significant reduction in cell viability (P < 0.001 vs no treatment group). The effect of uncleaved OTf (OTf) at 250 μg/mL is shown on the left (open bars) of the graphs. Values are the mean of three experiments from four parallel wells per sample in each experiment.

Rac-OTf Specifically Inhibits the Proliferation of Human Cancer Cells. In contrast to the marginal effect of intact OTf (Figure **2A**), rac-OTf caused a significant suppression of proliferation in both human breast (MCF-7) and human colon (HCT-116) cancer cell lines in a dose-dependent manner up to 500 μg/mL and then reached a plateau (**Figure 2B**). The rac-OTf showed no remarkable effect on the proliferation of normal human breast cell line HMEC (**Figure 2B**). The antiproliferation effect of rac-OTf displayed the most potency against HCT-116 compared with its effect on MCF-7. These results demonstrate that the rac-OTf confers antiproliferative activity against cancer cells and are in agreement with previous reports on different anticancer proteins, which are known to undergo autocleavage upon reduction (*6*,*39*).

Rac-OTf Is Cytotoxic to Human Cancer Cells. In an attempt to address whether the antiproliferative effect of rac-OTf is unique to growth inhibition or a cytotoxic action, we thus assessed its effect on the viability of the most sensitive cells, HCT-116 (Figure **3**). To ensure the validity of our investigation, two methods of evaluation were employed: the traditional vital cytoplasmic stain (TB exclusion) assay (**Figure 3A**) and a highly sensitive fluorescence-based cell viability assay (live/dead cytotoxicity) assay at different concentrations of rac-OTf (**Figure 3B**). In the TB exclusion assay, the intact OTf (250 μg/mL) exhibited a very weak effect (**Figure 3A**, OTf), whereas rac-OTf dramatically reduced viability of HCT-116 carcinoma cells in a dose-dependent manner; however, at 250 μg/mL viability was decreased to 45% (**Figure 3A**). Rac-OTf did not exhibit cytotoxicity against normal HMEC cell line, whereas its effect was almost similar to mock-treated cells (**Figure 3A**, inset). When the fluorescence-based assay was employed, rac-OTf showed potent cytotoxic activity in a dose-dependent manner, as indicated by the decrease in green (live) against red (dead) fluorescence (**Figure 3B**). It should be noted that the difference in the values between the two cytotoxicity methods employed in this study (**Figure 3**) is attributed to the basis of each assay and the level of fluorescence signals. In the traditional TB exclusion, live cells exclude the dye as the membrane is impermeable, but dead cells uptake the dye due to the lack of an intact cell membrane, whereas the data are directly presented as blue-stained dead cells. In the fluorescence-based assay, the kit comprises two probes: cal-AM and EthD-1, whereas EthD-1 is not able to penetrate intact cell membranes but adheres to nucleic acids of damaged (dead) cells to red-fluorescent product. Cal-AM usually produces a low signal of fluorescence because it needs to be hydrolyzed (activated) intracellularly by esterase to a green-fluorescent product (calcein); thus, green fluorescence is an indicator of esterase activity (live and dead cells) as well as cells that have intact membrane. Furthermore, the values in fluorometric assays are also affected by intrinsic cellular autofluorescence background, commonly caused by NADH, riboflavin, and flavoenzymes. The emission of these autofluorescent molecules is broad (500−700 nm) when excited in the blue (485 nm) region and overlaps emission of the used fluorochrome (*40*). Because the effect of the intact OTf on the proliferation (**Figure 2A**) and viability (**Figure 3**) was remarkably weaker than the effect of rac-OTf, the antitumor activity could be attributed to the released autoproteolytic fragments rather than the remaining unproteolyzed OTf (30%) in the rac-OTf preparation (**Figure 1Aa**, pH 4.0).

Morphological observation of HCT-116 cells indicated significant morphological differences between cells treated with rac-OTf, intact OTf, and mock-treated cells (Figure **4**). Of particular interest, HCT-116 cells treated with rac-OTf, whether confluent (**Figure 4A**) or nonadherent cells (**Figure 4B**), exhibited characteristics of cells undergoing apoptosis with comparable effect to that of the apoptosis inducer (camptothecin). It is worth noting that rac-OTf did not exhibit cytotoxicity against normal HMEC cell line, whereas its effect was almost similar to mock-treated cells

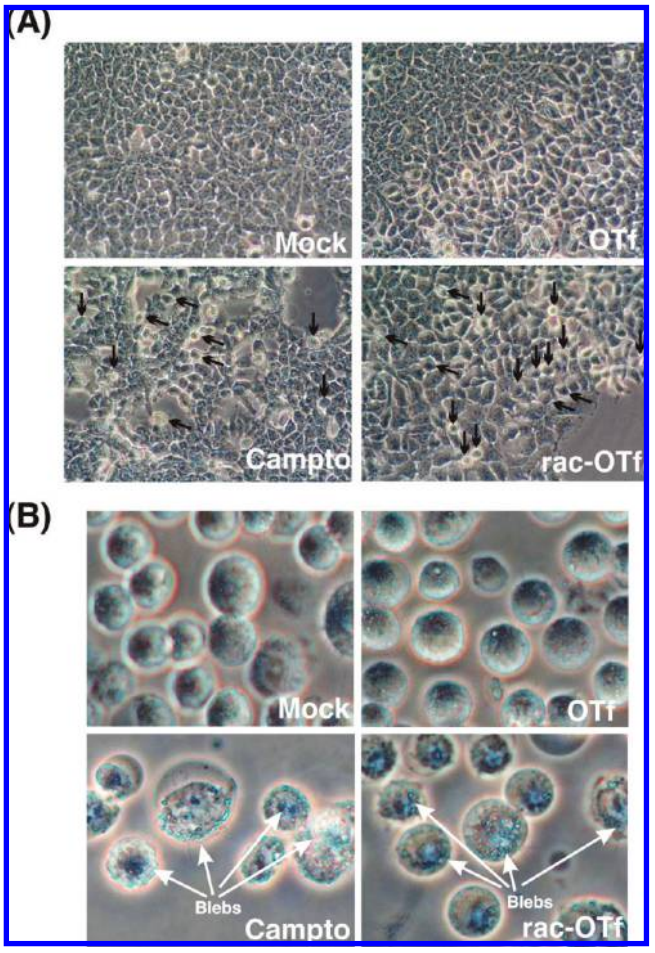

Figure 4. Effects of rac-OTf on HCT-116 cancer cell morphology. Cells were treated with OTf, rac-OTf, and camptothecin (Campto), an apoptosis inducer, for 4 h before (**A**) and after (**B**) detachment. Mock cells were treated with medium lacking additive as control. Cell morphology was observed by phase contrast microscopy at 100× (**A**) and 400× (**B**) magnification. Attached cells (**A**) treated with rac-OTf, OTf, and camptothecin displayed cell shrinkage, a rounded morphology, and increased detachment (black arrows). Nonadherent cells (**B**) treated with rac-OTf and camptothecin displayed blebs (white arrows), characteristic of apoptosis.

(**Figure 3A**), which is in a good agreement with its effect on proliferation (**Figure 2B**). To examine whether apoptotic killing is a relevant operative mechanism in the cytotoxic activity of rac-OTf against cancer cells, several bioassays were employed.

Antitumor Activity of Rac-OTf Is an Apoptosis-Mediated Action. The annexin V−EGFP (stain phosphatidylserine residues)/PI (stain DNA) dual staining assay was used to detect apoptotic cells. Positive staining with annexin V−EGFP (green RFU) correlates with loss of membrane polarity (exposure of phosphatidylserine to the outer surface). In contrast, PI can enter cells only after loss of membrane integrity. Thus, dual staining with annexin-V and PI allows clear discrimination between unaffected cells and apoptotic cells. As shown in Figure **5**, upon treatment of HCT-116 cells with camptothecin and rac-OTf, the green fluorescence (annexin-V positive) was increased 3.7- and 3.6-fold, respectively, over that of mock-treated cells (**Figure 5A**). In parallel, treatment with camptothecin and rac-OTf showed increase in the PI fluorescence to 13.5- and 21-fold, respectively, over that of mock-treated cells (**Figure 5B**). The results indicate that cells treated with rac-OTf were in the early stage of apoptosis (annexin-V positive), and a considerable number of cells were in

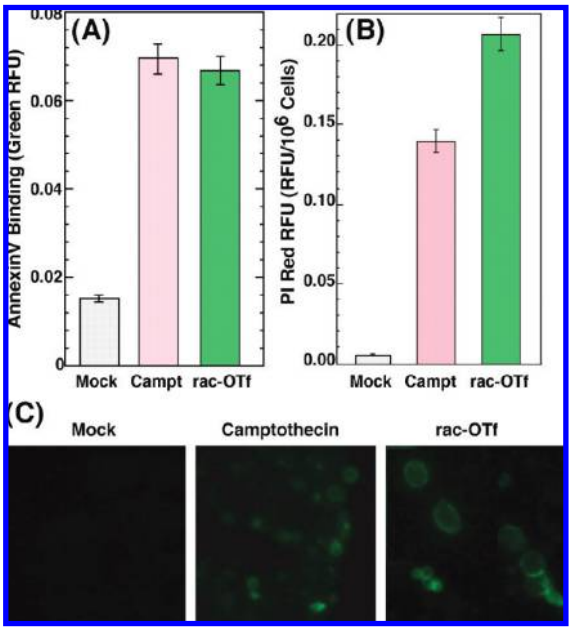

Figure 5. Induction of HCT-116 apoptosis by rac-OTf. Apoptosis was determined by staining the cells with annexin V−fluorescein (**A**) and propidium iodide (**B**). Data are expressed as relative fluorescence units of green (**A**) and red (**B**) fluorescence per 10^6 cells, after treatment with rac-OTf or camptothecin for 4 h. Values are the mean of two experiments from four parallel wells per sample in each experiment. Visualization of apoptotic cells (annexin-V positive) is also observed by fluorescent microscope at 200× magnification, and representative results are shown (**C**).

the late stage of apoptosis (PI positive). The annexin-V fluorescent staining of rac-OTf-treated cells, compared to the mock- and camptothecin-treated cells, was further confirmed by fluorescent microscope (**Figure 5C**).

Rac-OTf Induces the Loss of Mitochondrial Membrane Potential ($\Delta\Psi_m$). $\Delta\Psi_m$ was monitored in rac-OTf-treated HCT-116 cells using the cell-permeant, cationic fluorescent dye JC-1. Once inside a healthy nonapoptotic cell, the JC-1 dye enters the active mitochondria, where it aggregates and fluoresces red-orange. When the mitochondrial $\Delta\Psi_m$ collapses (in apoptotic cells), the dye is distributed throughout the cell as a monomeric form that fluoresces green. As shown in Figure **6A**, the proportion of JC-1-positive cells (green) relative to the mock-treated cells was increased following rac-OTf treatment with comparable effect to the camptothecin-treated cells. A fluorescent microscope was also employed to visualize the intracellular levels of the aggregated (red-orange) and monomeric (green) JC-1 dye (**Figure 6B**). Treatment with rac-OTf showed a decreased number of cells with active mitochondria (**Figure 6B**, white arrows) and increased green fluorescent cells, indicating the collapse of mitochondria $\Delta\psi_m$, whereas it is the point of the commitment of apoptosis.

Rac-OTf Induces the Activation of the Death Signals Caspases. The activation of caspase-6 and -9 plays the central role in the apoptotic death signal. The effect of rac-OTf on the activation of caspase-6 and -9 was investigated in HCT-116 as well as MCF-7 cells (Figure **7**). The intracellular activities of caspase-6 and -9 were greatly increased by treatment with rac-OTf or camptothecin in both cancer cell lines (**Figure 7A**). Upon exposure to rac-OTf, the activity of cytosolic caspase-6 and -9 increased to 2.5-fold in HCT-116, whereas in MCF-7 the activity increased to 7-fold that of mock-treated cells (**Figure 7B**). Although cells treated with OTf showed some increase in caspase activities, the activities were much pronounced in rac-OTf-treated cells, even

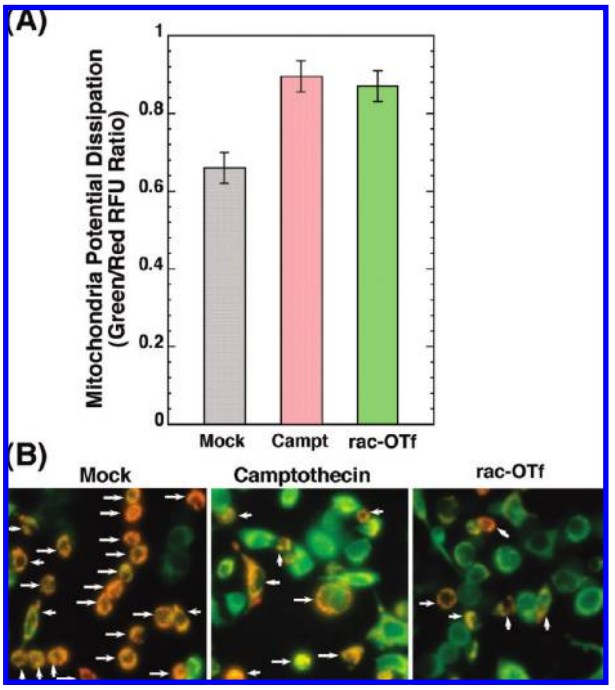

Figure 6. Dissipation of mitochondrial membrane potential of HCT-116 by rac-OTf. Membrane potential ($\Delta\Psi_m$) of mitochondria was determined by staining the cells with a redox-sensitive fluorescent probe that fluoresces red-orange when $\Delta\Psi_m$ is active and fluoresces green when $\Delta\Psi_m$ is collapsed. (**A**) Data are represented as relative fluorescence units of green/red ratios per 10^6 cells, after treatment with rac-OTf or camptothecin for 3.5 h. Values are the mean of two experiments from four parallel wells per sample in each experiment. (**B**) Collapse of mitochondria $\Delta\Psi_m$ was also visualized by fluorescent microscopy at 200× magnification. Arrows indicate cells with active $\Delta\Psi_m$.

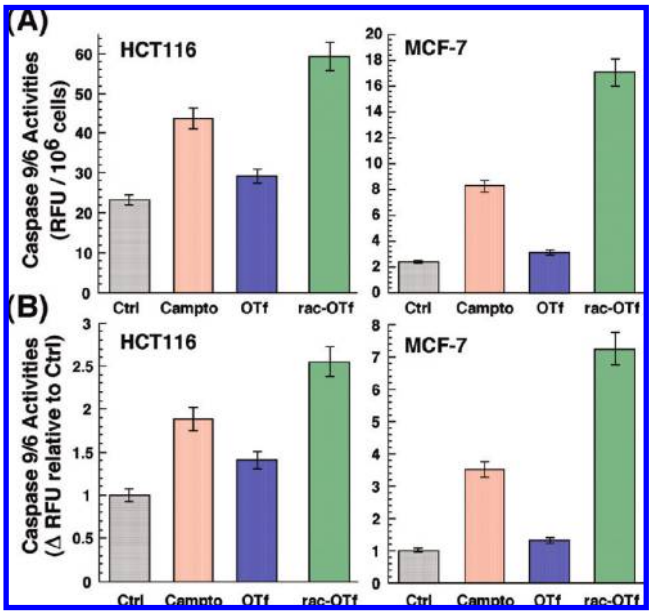

Figure 7. Caspase-9/-6 activation in HCT-116 and MCF-7 carcinoma cells by rac-OTf. Intracellular activity of caspase -9 and -6 was determined using cleavage assay of fluorometric substrate (LEHD-AMC) in lysates of treated cells with camptothecin, OTf, or rac-OTf for 1 h. Controls (Ctrl) contained medium without additive. Total cell count per each treatment was estimated in a hemocytometer under a microscope. The caspase activities are expressed as relative fluorogenic units (RFU) per 10^6 cells (**A**) and as fluorescence change over control (**B**). Values are the mean of three experiments from four parallel wells per sample in each experiment.

greater than the camptothecin-treated cells. Taken together, the results indicate that the reduction-induced autocleavage is a molecular switch responsible for the generation of a cytotoxic OTf form against cancer cells, whereas the lethal action operates through a mitochondria-mediated apoptotic pathway.

DISCUSSION

Our recent study demonstrated that the reduced autocleaved OTf exhibits more potent SOD-like activity (*30*). A surprising aspect is the absolute conservation throughout the autocleavage sites upstream of the kringle domains, which also falls within a region of the highest degree of sequence conservation in all transferrins (*19*). This redox-mediated autocleavage may be an important regulatory point in the physiologic and pathologic settings of OTf. This autocleavage mechanism of OTf mimics the process in which multiple antitumor kringles (angiostatins) are generated from plasmin(ogen). The goal of this study was to determine whether the reduced autocleaved OTf would inhibit the growth of cancer cells.

This work demonstrates, for the first time, that the autocleavage of OTf is a key process in the generation of multiple fragments with antitumor activity toward colon and breast cancer cells. The approach was facilitated by the autocleavage induced by a non-thiol reductant (TCEP), which produced highly resolved fragments (**Figure 1**). Interestingly, the acidic pH 4.0 generated a highly resolved autocleavage pattern of OTf when resolved on either reducing or nonreducing SDS-PAGE, indicating the correct intramolecular disulfide rearrangement in the self-cleaved domains. These results are consistent with the well-known extracellular acidic pH, which was maintained by the membrane proton pump (H^+-ATPase), and the extracellular disulfide-reducing condition of cancer cells (*41*, *42*). Whereas the uncleaved OTf showed marginal effect (**Figure 2A**), the rac-OTf inhibited the proliferation, dose dependently, of two human cancer cell lines, breast (MCF-7) and colon (HCT-116) cancers, without remarkable effect on the normal HMEC cells (**Figure 2B**). Particularly, rac-OTf exhibited remarkable cytotoxicity, dose dependently, against the most sensitive cancer cells, HCT-116, whereas it had no effect on normal HMEC cells (**Figure 3A**, inset).

The induction of apoptosis by defense peptides has been described in several cell types (*15*, *20*, *43*). Microscopic observation demonstrates that rac-OTf induced apoptosis of either adherent or nonadherent HCT-116 cells with similar effect to the apoptosis inducer camptothecin (**Figure 4**). A rapid onset of apoptosis of HCT-116 was confirmed by increased binding of annexin-V to phosphatidylserine exposed on the membrane of apoptotic cells and by fluorescence staining of cells with propidium iodide (**Figure 5**). In addition, we found that rac-OTf was able to cause loss in mitochondrial membrane potential ($\Delta\Psi_m$) of HCT-116 (**Figure 6**). These results suggest massive induction of apoptosis by rac-OTf comparable to the effect of camptothecin. Central to the execution of apoptosis is the permeabilization of the mitochondrial membrane with subsequent release of several pro-apoptotic factors into the cytosol (*44*). One of these factors, cytochrome *c*, alters the conformation of the cytosolic protein apoptotic protease activating factor-1 (APAF-1), whereupon this protein oligomerizes with pro-caspase-9 into the so-called apoptosome. Pro-caspase-9 is then autoproteolytically processed to caspase-9 and subsequently activates the executioner caspases, caspases-3, -6, and -7 (*45*, *46*). The activation of cytosolic caspase-6 and -9 by rac-OTf in two cancer cell lines, HCT-116 and MCF-7

(**Figure 7**), demonstrates that its cytotoxic action is mediated through mitochondria-mediated apoptotic pathway.

In conclusion, our results explore the importance of autoprocessing under reducing condition on the novel antitumor action of OTf, with particular emphasis on its defense role in the highly redox active milieu of cancer cells. The susceptibility of two different carcinoma cells to the rac-OTf was associated with apoptosis through the mitochondria pathway. As shown in our earlier study, the unique autoprocessing of OTf was attributed to the generation of multiple structural motifs strictly confined to both kringle domains (*19*). Cleavage of OTf occurred essentially at four distinct autocleavage motifs, flanking the two kringle domains of the N-lobe (nKGL) and C-lobe (cKGL). Mass spectrometry (MS/MS) analysis of the autoproteolytic peptides showed that all fragments were virtually generated by cleavage at the N-terminus of a Thr residue in the conserved "SCHT" and "CHT or HST" sequences, which correspond to the sequences 114−117, 210−212, 453−456, and 542−544, respectively, of OTf. The absolute conservation of the SCHT motif upstream of the two kringles and the HTT or HST motif downstream of the kringles thus perfectly releases the two kringles (residues 114−211 for nKGL and 455−543 for cKGL) or the central domain between them with one or both kringles, which may constitute a conserved regulatory domain. Hence, the reduction-mediated autoprocessing may be an important regulatory point in the physiologic and pathologic settings, allowing a portion of OTf to release biologically functional domains present in all members of the Tfs family (*19*) as reported in plasminogen (*29*). This finding is worthy when considering that the extracellular pH of tumors is acidic (*33*, *34*), and cancer cells are known for their high secretion of reducing agents and enzymes (*36*, *41*). We found the autoproteolytic fragments are tightly associated with each other and were difficult to isolate without severe structural damage; therefore, further genetic work will be required to determine the roles of the individual peptides in the anticancer action of OTf. The initial surprise occasioned by the novel discovery of this study that reduction-dependent autoprocessing converts OTf into an anticancer molecule thus seems likely to be joined by additional surprises as the role of the individual fragments is further elucidated. Eventually, the findings presented in this study provide new information on a novel biological function of OTf and offer a fascinating opportunity in the potential use of the reduced OTf in functional foods and as therapy for the treatment of cancers.

ABBREVIATIONS USED

OTf, ovotransferrin (hen egg albumin); rac-OTf, reduced autocleaved OTf; DTT, dithiothreitol; TCEP, tris(2-carboxyethyl)-phosphine (non-thiol reducing agent); ROS, reactive oxygen species; TB, trypan blue; PI, propidium iodide; cal-AM, calcein-AM; EthD-1, ethidium homodimer; JC-1, 5,5′,6,6′-tetrachloro-1,1′,3,3′-tetraethylbenzimidazolcarbocyanine iodide.

ACKNOWLEDGMENT

This work was supported in-part by Research Grant (KAKENHI-18580124) from the Ministry of Education, Culture, Sports, Science and Technology of Japan.

LITERATURE CITED

(1) Boonacker, E.; Van Noorden, C. J. The multifunctional or moonlighting protein CD26/DPPIV. *Eur. J. Cell Biol.* **2003**, *82* (2), 53–73.
(2) Jeffery, C. J. Moonlighting proteins: old proteins learning new tricks. *Trends Genet.* **2003**, *19* (8), 415–417.
(3) Perler, F. B.; Xu, M. Q.; Paulus, H. Protein splicing and autoproteolysis mechanisms. *Curr. Opin. Chem. Biol.* **1997**, *1* (3), 292–299.
(4) Perler, F. B. Protein splicing of inteins and hedgehog autoproteolysis: structure, function, and evolution. *Cell* **1998**, *92* (1), 1–4.
(5) Lee, J. J.; Ekker, S. C.; von Kessler, D. P.; Porter, J. A.; Sun, B. I.; Beachy, P. A. Autoproteolysis in hedgehog protein biogenesis. *Science* **1994**, *266* (5190), 1528–1537.
(6) Stathakis, P.; Lay, A. J.; Fitzgerald, M.; Schlieker, C.; Matthias, L. J.; Hogg, P. J. Angiostatin formation involves disulfide bond reduction and proteolysis in kringle 5 of plasmin. *J. Biol. Chem.* **1999**, *274* (13), 8910–8916.
(7) Davis, D. A.; Dorsey, K.; Wingfield, P. T.; Stahl, S. J.; Kaufman, J.; Fales, H. M.; Levine, R. L. Regulation of HIV-1 protease activity through cysteine modification. *Biochemistry* **1996**, *35*, 2482–2488.
(8) Smith, G. K.; Barrett, D. G.; Blackburn, K.; Cory, M.; Dallas, W. S.; Davis, R.; Hassler, D.; McConnell, R.; Moyer, M.; Weaver, K. Expression, preparation, and high-throughput screening of caspase-8: discovery of redox-based and steroid diacid inhibition. *Arch. Biochem. Biophys.* **2002**, *399* (2), 195–205.
(9) Kim, J. S.; Chang, J. H.; Yu, H. K.; Ahn, J. H.; Yum, J. S.; Lee, S. K.; Jung, K. H.; Park, D. H.; Yoon, Y.; Byun, S. M.; Chung, S. I. Inhibition of angiogenesis and angiogenesis-dependent tumor growth by the cryptic kringle fragments of human apolipoprotein. *J. Biol. Chem.* **2003**, *278* (31), 29000–29008.
(10) Shim, B. S.; Kang, B. H.; Hong, Y. K.; Kim, H. K.; Lee, I. H.; Lee, S. Y.; Lee, Y. J.; Lee, S. K.; Joe, Y. A. The kringle domain of tissue-type plasminogen activator inhibits in vivo tumor growth. *Biochem. Biophys. Res. Commun.* **2005**, *327* (4), 1155–1162.
(11) Wang, H.; Schultz, R.; Hong, J.; Cundiff, D. L.; Jiang, K.; Soff, G. A. Cell surface-dependent generation of angiostatin 4.5. *Cancer Res.* **2004**, *64* (1), 162–168.
(12) Lucas, R.; Holmgren, L.; Garcia, I.; Jimenez, B.; Mandriota, S. J.; Borlat, F.; Sim, B. K.; Wu, Z.; Grau, G. E.; Shing, Y.; Soff, G. A.; Bouck, N.; Pepper, M. S. Multiple forms of angiostatin induce apoptosis in endothelial cells. *Blood* **1998**, *92* (12), 4730–4741.
(13) Ibrahim, H. R. Ovotransferrin: chemistry and antimicrobial function. In *Natural Food Antimicrobial Systems*; Naidu, A. S., Ed.; CRC Press: Boca Raton, FL, 2000; pp 211−226.
(14) Carlevaro, M. F.; Albini, A.; Ribatti, D.; Gentili, C.; Benelli, R.; Cermelli, S.; Cancedda, R.; Cancedda, F. D. Transferrin promotes endothelial cell migration and invasion: implication in cartilage neovascularization. *J. Cell Biol.* **1997**, *136* (6), 1375–1384.
(15) Furlong, S. J.; Mader, J. S.; Hoskin, D. W. Lactoferricin-induced apoptosis in estrogen-nonresponsive MDA-MB-435 breast cancer cells is enhanced by C6 ceramide or tamoxifen. *Oncol. Rep.* **2006**, *15* (5), 1385–1390.
(16) Mader, J. S.; Salsman, J.; Conrad, D. M.; Hoskin, D. W. Bovine lactoferricin selectively induces apoptosis in human leukemia and carcinoma cell lines. *Mol. Cancer Ther.* **2005**, *4* (4), 612–624.
(17) Sala, R.; Jefferies, W. A.; Walker, B.; Yang, J.; Tiong, J.; Law, S. K.; Carlevaro, M. F.; Di Marco, E.; Vacca, A.; Cancedda, R.; Cancedda, F. D.; Ribatti, D. The human melanoma associated protein melanotransferrin promotes endothelial cell migration and angiogenesis in vivo. *Eur. J. Cell Biol.* **2002**, *81* (11), 599–607.
(18) Xie, H.; Huff, G. R.; Huff, W. E.; Balog, J. M.; Rath, N. C. Effects of ovotransferrin on chicken macrophages and heterophil-granulocytes. *Dev. Comp. Immunol.* **2002**, *26* (9), 805–815.
(19) Ibrahim, H. R.; Haraguchi, T.; Aoki, T. Ovotransferrin is a redox-dependent autoprocessing protein incorporating four consensus self-cleaving motifs flanking the two kringles. *Biochim. Biophys. Acta* **2006**, *1760* (3), 347–355.
(20) Gogvadze, V.; Sten Orrenius, S.; Zhivotovsky, B. Mitochondria in cancer cells: what is so special about them? *Trends Cell Biol.* **2008**, *18* (4), 165–173.
(21) Gillies, R. J.; Gatenby, R. A. Adaptive landscapes and emergent phenotypes: why do cancers have high glycolysis? *J. Bioenerg. Biomembr.* **2007**, *39*, 251–257.
(22) Stafforda, J. L.; Belosevica, M. Transferrin and the innate immune response of fish: identification of a novel mechanism of macrophage activation. *Dev. Comp. Immunol.* **2003**, *27*, 539–554.
(23) Xiao, Y.; Monitto, C. L.; Minhas, K. M.; Sidransky, D. Lactoferrin down-regulates G1 cyclin-dependent kinases during growth arrest of head and neck cancer cells. *Clin. Cancer Res.* **2004**, *10* (24), 8683–8686.

(24) Wolf, J. S.; Li, G.; Varadhachary, A.; Petrak, K.; Schneyer, M.; Li, D.; Ongkasuwan, J.; Zhang, X.; Taylor, R. J.; Strome, S. E.; O'Malley, B. W.Jr. Oral lactoferrin results in T cell-dependent tumor inhibition of head and neck squamous cell carcinoma in vivo. *Clin. Cancer Res.* **2007**, *13* (5), 1601–1610.

(25) Chandra Mohan, K. V.; Kumaraguruparan, R.; Prathiba, D.; Nagini, S. Modulation of xenobiotic-metabolizing enzymes and redox status during chemoprevention of hamster buccal carcinogenesis by bovine lactoferrin. *Nutrition* **2006**, *22* (9), 940–946.

(26) Baumrucker, C. R.; Schanbacher, F.; Shang, Y.; Green, M. H. Lactoferrin interaction with retinoid signaling: cell growth and apoptosis in mammary cells. *Domest. Anim. Endocrinol.* **2006**, *30* (4), 289–303.

(27) Richardson, D. R.; Baker, E. The uptake of iron and transferrin by the human malignant melanoma cell. *Biochim. Biophys. Acta* **1990**, *1053*, 1–12.

(28) Leveugle, B.; Spik, G.; Perl, D. P.; Bouras, C.; Fillit, H. M.; Hof, P. R. The iron-binding protein lactotransferrin is present in pathologic lesions in a variety of neurodegenerative disorders: a comparative immunohistochemical analysis. *Brain Res.* **1994**, *650*, 20–31.

(29) Davidson, D. J.; Haskell, C.; Majest, S.; Kherzai, A.; Egan, D. A.; Walter, K. A.; Schneider, A.; Gubbins, E. F.; Solomon, L.; Chen, Z.; Lesniewski, R.; Henkin, J. Kringle 5 of human plasminogen induces apoptosis of endothelial and tumor cells through surface-expressed glucose-regulated protein 78. *Cancer Res.* **2005**, *65* (11), 4663–4672.

(30) Ibrahim, H. R.; Hoq, M. I.; Aoki, T. Ovotransferrin possesses SOD-like superoxide anion scavenging activity that is promoted by copper and manganese binding. *Int. J. Biol. Macromol.* **2007**, *41* (5), 631–640.

(31) Weydert, C. J.; Zhang, Y.; Sun, W.; Waugh, T. A.; Teoh, M. L.; Andringa, K. K.; Aykin-Burns, N.; Spitz, D. R.; Smith, B. J.; Oberley, L. W. Increased oxidative stress created by adenoviral MnSOD or CuZnSOD plus BCNU (1,3-bis(2-chloroethyl)-1-nitrosourea) inhibits breast cancer cell growth. *Free Radical Biol. Med.* **2008**, *44* (5), 856–867.

(32) Weydert, C. J.; Waugh, T. A.; Ritchie, J. M.; Iyer, K. S.; Smith, J. L.; Li, L.; Spitz, D. R.; Oberley, L. W. Overexpression of manganese or copper−zinc superoxide dismutase inhibits breast cancer growth. *Free Radical Biol. Med.* **2006**, *41*, 226–237.

(33) Raghunand, N.; Altbach, M. I.; Sluis, R. V.; Baggett, B.; Taylor, C. W.; Bhujwalla, Z. M.; Gillies, R. J. Plasmalemmal pH-gradients in drug-sensitive and drug-resistant MCF-7 human breast carcinoma xenografts measured by ^{31}P magnetic resonance spectroscopy. *Biochem. Pharmacol.* **1999**, *57*, 309–312.

(34) Wike-Hooley, J. L.; Haveman, J.; Reinhold, H. S. The relevance of tumour pH to the treatment of malignant disease. *Radiother. Oncol.* **1984**, *2*, 343–366.

(35) Stathakis, P.; Fitzgerald, M.; Matthias, L. J.; Chesterman, C. N.; Hogg, P. J. Generation of angiostatin by reduction and proteolysis of plasmin. Catalysis by a plasmin reductase secreted by cultured cells. *J. Biol. Chem.* **1997**, *272* (33), 20641–20645.

(36) Lincoln, D. T.; Ali Emadi, E. M.; Tonissen, K. F.; Clarke, F. M. The thioredoxin-thioredixin reductase system: over-expression in human cabcer. *Anticancer Res.* **2003**, *23* (3B), 2425–2433.

(37) Bradshaw, T. D.; Matthews, C. S.; Cookson, J.; Chew, E. H.; Shah, M.; Bailey, K.; Monks, A.; Harris, E.; Westwell, A. D.; Wells, G.; Laughton, C. A.; Stevens, M. F. Elucidation of thioredoxin as a molecular target for antitumor quinols. *Cancer Res.* **2005**, *65*, 3911–3919.

(38) Chew, E. H.; Lu, J.; Bradshaw, T. D.; Holmgren, A. Thioredoxin reductase inhibition by antitumor quinols: a quinol pharmacophore effect correlating to antiproliferative activity. *FASEB J.* **2008**, *22*, 2072–2083.

(39) Yang, X.; Cheng, R.; Li, C.; Cai, W.; Ma, J. X.; Liu, Q.; Yang, Z.; Song, Z.; Liu, Z.; Gao, G. Kringle 5 of human plasminogen suppresses hepatocellular carcinoma growth both in grafted and xenografted mice by anti-angiogenic activity. *Cancer Biol. Ther.* **2006**, *5* (4), 399–405.

(40) Victoria, L.; Mosiman, V. L.; Patterson, B. K.; Canterero, L.; Goolsby, C. L. Reducing cellular autofluorescence in flow cytometry: an in situ method. *Cytometry* **1997**, *30*, 151–156.

(41) Morikawa, W.; Yamamoto, K.; Ishikawa, S.; Takemoto, S.; Ono, M.; Fukushi, J.; Naito, S.; Nozaki, C.; Iwanaga, S.; Kuwano, M. Angiostatin generation by cathepsin D secreted by human prostate carcinoma cells. *J. Biol. Chem.* **2000**, *275* (49), 38912–38920.

(42) Tannock, I. F. Response of aerobic and hypoxic cells in a solid tumor to Adriamycin and cyclophosphamide and interaction of the drugs with radiation. *Cancer Res.* **1982**, *42*, 4921–4926.

(43) Mader, J. S.; Hoskin, D. W. Cationic antimicrobial peptides as novel cytotoxic agents for cancer treatment. *Expert Opin. Invest. Drugs* **2006**, *15* (8), 933–946.

(44) Chen, T.; Wong, Y.-S. Selenocystine induces caspase-independent apoptosis in MCF-7 human breast carcinoma cells with involvement of p53 phosphorylation and reactive oxygen species generation. *Intl. J. Biochem. Cell Biol.* **2009**, *41*, 666–676.

(45) Ghobrial, I. M.; Witzig, T. E.; Adjei, A. A. Targeting apoptosis pathways in cancer therapy. *CA Cancer J. Clin.* **2005**, *55*, 178–194.

(46) Kim, R. Recent advances in understanding the cell death pathways activated by anticancer therapy. *Cancer* **2005**, *103*, 1551–1560.

Received for review July 29, 2009. Revised manuscript received September 30, 2009. Accepted October 14, 2009.